Meteoritic highly siderophile element and Re-Os isotope signatures of Archean spherule layers from the CT3 drill core, Barberton Greenstone Belt, South Africa

Seda OZDEMIR [1*], Toni SCHULZ[1,2], David van ACKEN[3], Ambre LUGUET[4],
W. Uwe REIMOLD [5], and Christian KOEBERL [1,6*]

[1]Department of Lithospheric Research, University Vienna, Althanstrasse 14, 1090 Vienna, Austria
[2]Institut für Geologie und Mineralogie, University Cologne, Zülpicher Strasse 49a, 50674 Cologne, Germany
[3]Irish Centre for Research in Applied Geosciences (iCRAG), UCD School of Earth Sciences, University College Dublin, Belfield, Dublin 4, Ireland
[4]Steinmann-Institut of Geology, Mineralogy and Palaeontology, University of Bonn, Poppelsdorfer Schloss, 53115 Bonn, Germany
[5]Geochronology Laboratory, Instituto de Geociências, Universidade de Brasília, 70910-900 Brasília, DF, Brazil
[6]Natural History Museum, Burgring 7, A-1010 Vienna, Austria
[*]Corresponding author. E-mails: seda.oezdemir@univie.ac.at or christian.koeberl@univie.ac.at

Abstract–Archean spherule layers represent the only currently known remnants of the early impact record on Earth. Based on the lunar cratering record, the small number of spherule layers identified so far contrasts to the high impact flux that can be expected for the Earth at that time. The recent discovery of several Paleoarchean spherule layers in the BARB5 and CT3 drill cores from the Barberton area, South Africa, drastically increases the number of known Archean impact spherule layers and may provide a unique opportunity to improve our knowledge of the impact record on the early Earth. This study is focused on the spherule layers in the CT3 drill core from the northeastern Barberton Greenstone Belt. We present highly siderophile element (HSE: Re, Os, Ir, Pt, Ru, and Pd) concentrations and Re-Os isotope signatures for spherule layer samples and their host rocks in order to unravel the potential presence of extraterrestrial fingerprints within them. Most spherule layer samples exhibit extreme enrichments in HSE concentrations of up to superchondritic abundances in conjunction with, in some cases, subchondritic present-day $^{187}Os/^{188}Os$ isotope ratios. This indicates a significant meteoritic contribution to the spherule layers. In contrast to some of the data reported earlier for other Archean spherule layers from the Barberton area, the CT3 core is significantly overprinted by secondary events. However, HSE and Re-Os isotope signatures presented in this study indicate chondritic admixtures of up to (and even above) 100% chondrite component in some of the analyzed spherule layers. There is no significant correlation between HSE abundances and respective spherule contents. Although strongly supporting the impact origin of these layers and the presence of significant meteoritic admixtures, peak HSE concentrations are difficult to explain without postdepositional enrichment processes.

INTRODUCTION

Because the Earth is geologically active, most of the ancient terrestrial impact structures have become obscured with time (the oldest known impact crater structure is the approximately 2 Ga old Vredefort structure; e.g., Reimold and Koeberl 2014). The only

evidence for Archean impact events on Earth comes in the form of distal ejecta in the form of strata bearing, or being strongly enriched in, impact-derived spherules (e.g., Lowe and Byerly 1986; Glass and Simonson 2013). Such extensive spherule deposits are rarely observed in relation to post-Archean impact events and provide (thanks to their local preservation over

extremely long periods of time) the only accessible tracers of the Early Archean impact record. Paleoarchean impact layers, with ages ranging from 3.4 to 3.2 Ga, have, so far, been identified in the Pilbara craton in Australia and the Barberton Greenstone Belt (BGB) in South Africa (e.g., Lowe and Byerly 1986; Shukolyukov et al. 2000; Simonson et al. 2000, 2009; Byerly et al. 2002; Lowe et al. 2003, 2014; Hofmann et al. 2006; Glass and Simonson 2013); some of these may well be correlated. Such correlations are typically based on stratigraphic considerations, as well as concurring zircon ages of sedimentary units in close proximity to the spherule layers. For example, an approximately 3470 Ma old spherule bed, preserved in the Pilbara Craton, is assumed to be correlated with another one of the same age in the Barberton Greenstone Belt (Byerly et al. 2002), suggesting that these spherule deposits may represent a single global fallout layer that is associated with sedimentation affected by an impact-generated tsunami.

It remains, however, poorly constrained how the so far known spherule beds from the Barberton Greenstone Belt are correlated among each other. After decades of debate about the enormous (up to slightly superchondritic) highly siderophile element (HSE: Re, Os, Ir, Pt, Ru, and Pd) enrichments in some of the Barberton spherule layers (Koeberl and Reimold 1995; Reimold et al. 2000), Kyte et al. (2003) and Shukolyukov et al. (2000) provided convincing evidence for an impact origin in the form of carbonaceous chondritic Cr isotope signatures in some of the analyzed spherule layers. The authors reported the presence of carbonaceous chondrite-like material, amounting to ~1%, 50–60%, and 15–30% in spherule layers S2, S3, and S4, respectively. Undoubtedly, these results provided a major boost for the impact hypothesis for Barberton spherule layers and were able to explain the chondritic HSE abundances. On the other hand, the concentrations above the chondritic HSE abundances and the values slightly below the chondritic HSE interelement ratios might best be explained by moderate postimpact hydrothermal overprint, or another alteration/concentration mechanism (see, e.g., discussion in Koeberl [2014] and Schulz et al. 2017; Mohr-Westheide et al. 2018).

Lowe and coworkers initially identified four (possibly up to eight) spherule layers (see, e.g., Lowe et al. 1989, 2003, 2014). Layer S1 is embedded in the predominantly volcanic Onverwacht group (Byerly et al. 2002) of the BGB and probably related to a Pilbara spherule layer in Western Australia (Simonson 1992). All other known Paleoarchean spherule layers occur within the sedimentary strata of the Fig Tree Group of the Barberton stratigraphy. Two recently drilled cores in the BGB (BARB5 and CT3) contain up to 21 spherule layer intersections. These, in all likelihood though represent fewer actual impact events, due to likely possible tectonic duplication and the need to group some intersections together into one layer (as discussed by Fritz et al. 2016; Ozdemir et al. 2017; and Hoehnel et al. 2018). In any case, all these spherule bed intersections occur in the Fig Tree Group and are of Paleoarchean age.

However, the high amounts of meteoritic component identified in many of the Barberton spherule layers separates these samples from more recent impact ejecta, which exhibit extraterrestrial admixtures that are orders of magnitude lower (see Koeberl 2014). Any such strong admixtures to the Barberton spherule layers should not only be identifiable by elevated (moderately and highly) siderophile element abundances (and the interelement ratios of these elements) but also by their ^{187}Os isotope signatures. The long-lived ^{187}Re-^{187}Os isotopic system (^{187}Re $\rightarrow$ ^{187}Os + β^- with a λ of 1.64×10^{-11} year^{-1}; Smoliar et al. 1996) is a significant tool for studying impact craters and their ejecta (e.g., Palme 1982; Koeberl and Shirey 1997; Koeberl 2007, 2014; Koeberl et al. 2012). Both Re and Os are siderophile elements. Due to the, compared to Os, more incompatible behavior of Re during mantle melting, Os is depleted within crustal material while Re is enriched (^{187}Re/^{188}Os ~50 for continental crust; Esser and Turekian [1993], compared to ~0.39 for chondrites; Shirey and Walker 1998). As a consequence, crustal material evolves to radiogenic ^{187}Os values over time (~1.4 for the average continental crust, compared to ~0.12 for chondrites; Peucker-Ehrenbrink and Jahn [2001] and Shirey and Walker [1998]). Together with the contrasting HSE contents between the average continental crust (ppt level; e.g., ~30 ppt Os; Peucker-Ehrenbrink and Jahn 2001) and chondrites (ppb level; e.g., ~500 ppb Os in CI chondrites; Tagle and Berlin 2008), the difference in ^{187}Os signatures provides the basis of the Re-Os isotope tool. Even tiny admixtures in the percent- and sub-percent level of extraterrestrial material to impactites lead to significant deviations from the ^{187}Os signatures of the typically crustal target material at impact sites. However, mafic target lithologies exhibit more mantle-like (and, thus, nearer to chondritic) ^{187}Os signatures, leading to less sensitive mixing relationships between the terrestrial and extraterrestrial endmembers. A careful petrographic inspection of the samples at the impact site is, thus, always a prerequisite in the discussion of both HSE abundances and ^{187}Os/^{188}Os isotope data of impactites.

Following detailed spectroscopic and petrochemical investigations, implying a single impact scenario for the BARB5 spherule layers (Fritz et al. 2016), Schulz et al.

(2017) reported HSE and Re-Os isotope data of these spherule layers, leading to the suggestion that up to three distinct impact events could be represented by the analyzed four spherule layers. However, an open debate remained as to whether or not some of these layers/events can be correlated with the S1 to S4 horizons (see Ozdemir et al. [2017] for the detailed explanation of these layers). In addition, a petrographic and geochemical studies by Ozdemir et al. (2017) and Hoehnel et al. (2018) on the CT3 core reported mineralogical and geochemical evidence for the existence of three spherule-bearing intervals, hosting up to 14 distinct spherule sections. It was discussed that they represent at least three different impact events. In order to further strengthen the conclusions drawn from this investigation, we here present concentrations of selected HSE in conjunction with [187]Os isotope signatures of both, spherule-bearing horizons and spherule-free host rocks from the CT3 core.

SAMPLES

All samples analyzed in this study were collected from the CT3 core, which was drilled through Fig Tree Group sediments in the northeastern BGB (for more detailed information, see, Ozdemir et al. [2017] and Hoehnel et al. [2018]). The latter authors reported that only Ni- rich Cr-spinel (up to 11 wt% NiO) crystals, rare zircon grains, and alloys of platinum group elements, which include also Fe and/or Ni, represent primary phases in these otherwise thoroughly altered strata of the CT3 spherule layer sections. Fifteen samples from all three spherule intervals of the CT3 core (as described in Ozdemir et al. 2017) were analyzed for their HSE concentrations using isotope dilution, and their [187]Os/[188]Os isotope ratios (Table 1). The samples include nine spherule layer samples (spherule-groundmass assemblages) and six country rock samples (mostly shales and cherts; see Ozdemir et al. [2017] for petrographic sample descriptions). We also performed replicate measurements of samples B-SH11 and B-SH19s. The analyzed samples and their positions within the spherule layer-hosting CT3 core sections are schematically shown in Fig. 1. Names of samples analyzed in this study are the same as those introduced in Ozdemir et al. (2017) and include the prefix A, B, or C (for the respective spherule layer interval of the CT3 core), SL (for spherule layer), SH (for shale), followed by numbers according to the sample positions within the drill core section (see Fig. 1). An "s" denotes samples containing sulfides. It should, in addition, be noted that all country rock samples from this study lie in close proximity to the next spherule layers. They are visibly free of spherules but are possibly affected by impact-related or postimpact element mobilization and diffusive interaction with the neighboring spherule layers. Moreover, the country rocks include Ni-rich chromium spinels (a suggested carrier phase of the meteoritic component in CT3 drill core; see Mohr-Westheide et al. 2018), which are either detached from spherules or included in tiny spherule fragments (see also explanations in Ozdemir et al. 2017).

The two lithologies analyzed in this study, country rocks and spherule layers are stratigraphically related to the Fig Tree Group, which contains shales, black shales, cherts, greywackes, and jaspilites (e.g., Hofmann 2005), all deposited between 3.2 and 3.5 Ga (Ozdemir et al. 2017). Average HSE data for Fig Tree Group sediments from the literature (Siebert et al. 2005) are shown in element correlation diagrams throughout this study, for comparison.

METHODS

[187]Os/[188]Os ratios and Os concentrations of the spiked samples were determined at the Department of Lithospheric Research at the University of Vienna, Austria, by using a ThermoFinnigan Triton thermal ionization mass spectrometer operating in negative ion mode. Between ~0.1 and ~0.6 g of homogenized sample (obtained from ∼2 g rock fragments cut with diamond saw blades from the quarter drill core sections) were spiked with a mixed tracer solution (enriched in [99]Ru, [105]Pd, [185]Re, [190]Os, [191]Ir, and [194]Pt). The sample-spike mixtures were then digested in 7 ml inverse aqua regia (HNO_3-HCl: 5 + 2 ml) at 250°C and 100–130 bars in an Anton-Paar high-pressure asher for 12 hours. Osmium and the other HSE were then separated according to the extraction procedures described in Cohen and Waters (1996). Osmium was further purified by microdistillation (Birck et al. 1997) and the other elements were separated using a procedure adapted from the method of Pearson and Woodland (2000). For mass spectrometric analysis, Os was loaded as a bromide ($OsBr_3$) on Pt ribbon filaments (0.02 mm thick, 1 mm wide) together with a saturated Na(OH)/Ba(OH)$_2$ activator solution (see Luguet et al. 2008). Osmium was measured as OsO_3 ions in a peak hopping mode using a secondary electron multiplier (SEM) detector. Isobaric interferences attributable to W- or Pt-oxide were not observed. Isobaric interferences of [187]Re on [187]Os were monitored by measuring [185]ReO$_3$ (mass 233) and were corrected for, if observed. Mass fractionation was corrected offline using [192]Os/[188]Os = 3.083 (Brandon et al. 2005; Luguet et al. 2008). The total Os procedural blank was ~6 ± 4 pg (n = 3), contributing less than 0.1% to most of the measured Os concentrations.
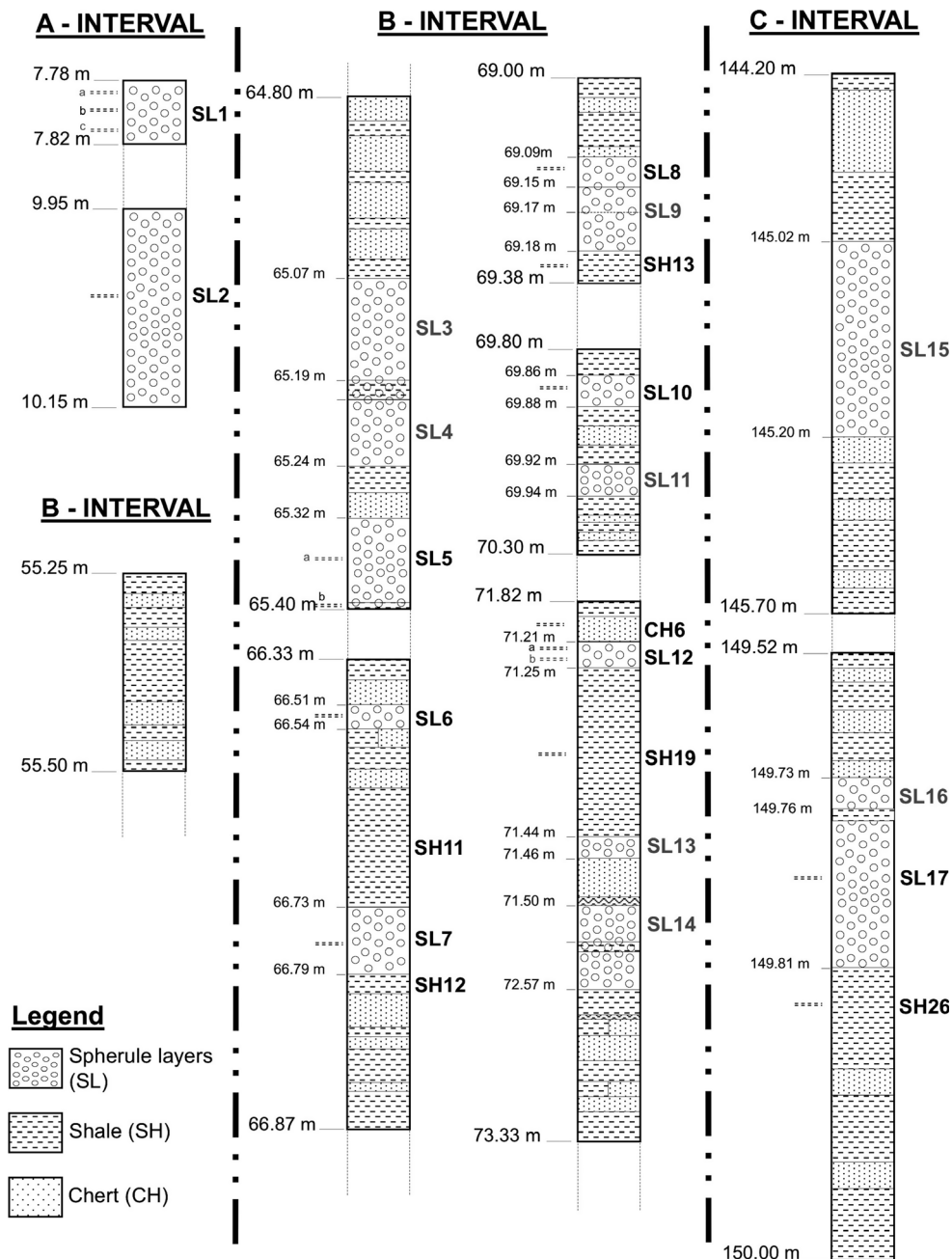
Fig. 1. Schematic stratigraphic column for the CT3 drill core intervals containing spherule layers and country rock layers (modified after Ozdemir et al. 2017). The layer names discussed in this work are written in black.

Rhenium, Ir, Pt, Ru, and Pd concentrations were determined using a Thermo Element XR SF-ICP-MS in single collector mode at the Steinmann-Institute at the University of Bonn, Germany, using methods described in Luguet et al. (2015). Total blanks for this study (n = 4) were ~4 pg for Re, ~3 pg for Ir, ~70 pg for Ru, ~22 pg for Pt, and ~50 pg for Pd. Due to the extremely high concentrations of HSE in most of the analyzed samples, blank corrections were mostly minor or

negligible. In the case of low-HSE concentrations (e.g., samples B-SH11-II or B-SL7), blank corrected values are reported.

RESULTS

Concentrations of HSE and $^{187}Os/^{188}Os$ isotope ratios for all analyzed samples are compiled in Table 1.

Table 1. Rhenium-Os isotope ratios and highly siderophile element (HSE) abundances of samples from the CT3 drill core sections.

Sample	Depth (m)	Os^a	Os^b	Ir^a	Ir^b	Ru^a	Pt^a	Pd^a	Re^a	$^{187}Re/^{188}Os$	$\pm2\sigma$	$^{187}Os/^{188}Os$	$\pm2\sigma$	$(^{187}Os/^{188}Os)_i$	$\pm2\sigma$
A-SL1b	7.79–7.80	12.51	–	6.21	6.83	–	148.6	–	0.10	0.0381	0.0011	0.1313	0.0032	0.1291	0.0032
A-SL2	9.95–10.15	18.10	–	6.72	9.03	–	20.51	–	0.45	0.1184	0.0036	0.12902	0.00032	0.12212	0.00032
B-SL5b	65.34–65.40	2721	1858	1931	2068	–	3778	4705	57.39	0.1001	0.0031	0.1130	0.0003	0.1072	0.0003
B-SL6	66.51–66.54	2.96	–	0.03	8.68	0.70	1.65	3.06	0.19	0.3072	0.0092	0.1668	0.0012	0.1481	0.0012
B-SH11-I	66.66–66.73	0.15	–	47.63	0.97	165.3	192.2	30.08	4.67	167.9	5.0	1.1265	0.0090	–	–
B-SH11-II	66.66–66.73	1.82	–	0.42	0.97	–	6.02	–	0.65	1.732	0.052	0.26642	0.00082	0.16549	0.00082
B-SL7	66.73–66.79	2.96	–	0.11	6.12	0.26	1.42	0.15	0.21	0.338	0.010	0.1341	0.0004	0.1144	0.0004
B-SH12s	66.79–66.83	0.11	–	3.93	0.59	10.78	16.14	5.17	0.11	4.820	0.140	0.2139	0.0022	–	–
B-SL8	69.09–69.16	2282	–	53.03	5.01	99.81	169.2	54.24	1.11	0.0023	0.0001	0.1128	0.0001	0.1127	0.0001
B-SH13	69.17–69.86	2372	–	–	2832	–	–	–	–	–	–	0.107946	0.0001	–	–
B-SL10s	69.86–69.88	966.7	1333	536.3	649.0	–	691.0	–	95.25	0.4700	0.0140	0.1422	0.0016	0.1148	0.0016
B-CH6s	70.86–71.21	18.20	–	–	12.90	–	–	–	–	–	–	0.32841	0.00032	–	–
B-SL12a	71.21–71.23	384.2	–	305.4	2.05	–	679.3	–	23.19	0.2876	0.0086	0.1319	0.0003	0.1152	0.0003
B-SH19s-I	71.25–71.44	2230	2413	2328	2619	–	3660	–	–	–	–	0.12569	0.00011	–	–
B-SH19s-II	71.25–71.44	2144	2413	2057	2619	–	3497	–	130.4	0.2895	0.0870	0.12569	0.00006	0.10882	0.00006
C-SL17	149.77–149.81	395.7	362	365.7	602.0	–	947.9	–	6.24	0.0749	0.0022	0.111173	0.000072	0.106810	0.000072
C-SH26	149.81–149.82	576.8	629	384.4	563.0	–	647.4	–	105.0	0.8740	0.0260	0.18762	0.00042	0.13671	0.00042
Chondrites		364.0–2850[c]		336.0–2635[c]			707.0–1596[c]		63.23–96.96[d]	0.3731–0.4779[e]		0.1238[f]–0.1304[e]		~0.1085[d]	
BARB5[g]		1.46–944.5		4.53–552.0			5.22–2082			0.0101–0.1464		0.1064–0.3161		0.1048	

[a] Concentrations obtained by isotope dilution (ID).
[b] Concentrations obtained by instrumental neutron activation analysis (INAA). All concentrations in ppb. $(^{187}Os/^{188}Os)_i$ = back-calculated.
[c] Tagle and Berlin (2008).
[d] Shirey and Walker (1998).
[e] Walker et al. (2002).
[f] Van Acken et al. (2011).
[g] Schulz et al. (2017).

Highly Siderophile Elements

Samples from spherule layers and country rocks exhibit similar HSE contents. The contents in the nine spherule layer samples vary from 0.03 to 1931 ppb for Ir, from ~3 to 2721 ppb for Os, from ~0.3 to ~100 ppb for Ru, from ~1.5 to 3778 ppb for Pt, from ~0.2 to 4705 ppb for Pd, and from ~0.1 to ~95 ppb for Re. In comparison, HSE abundances in the country rock samples range from ~0.4 to 2328 ppb for Ir, from ~0.1 to 2371 ppb for Os, from ~11 to ~165 ppb for Ru, from ~6 to 3559 ppb for Pt, from ~5 to ~30 for Pd, and from ~0.1 to ~130 ppb for Re. Notably, the highest HSE concentrations in CT3 samples are up to two orders of magnitude higher compared to contents observed in average Fig Tree Group sediments (Siebert et al. 2005) and, except for Re and as shown in Fig. 2, even higher than those measured in other spherule layers from the BGB. Other Archean spherule layers showed maximum Ir concentrations of 240 ppb in the S4 layer (Kyte et al. 1992), 1518 ppb in the S2 layer (Reimold et al. 2000), ~700 ppb in the S3 layer (Lowe et al. [2003] and references therein), 357 ppb in the Paraburdoo spherule layer (Goderis et al. 2013), 725 ppb in the S3 layer (Kyte et al. 2003), and 552 ppb in the BARB5 core (Schulz et al. 2017).

Schulz et al. (2017) reported a bimodality between BARB5 spherule and country rock layers, with a rough tendency of increasing HSE contents in samples with successively higher spherule contents. Moreover, Mohr-Westheide et al. (2015) and Fritz et al. (2016), reported a correlation between HSE contents and Ni-spinels within BARB5 samples and concluded that the Ni-spinels are the HSE carrier phases. Such, although rough, correlations between HSE contents and density of the spherules, could not be found for the CT3 samples analyzed in this study. Notably, a recent study by Mohr-Westheide et al. (2018) confirmed an association of HSE phases and Ni-Cr spinels in CT3 layers, which were found in spherule layers and country rocks (B-SL5b, B-SL8, B-SH13, B-SH19s, B-SL10, and C-SL17). They also presented HSE alloys as the reason of a nugget effect which causes these extreme HSE enrichments, together with secondary alterations such as HSE-bearing sulfarsenides observed in spinel fragments. Notably, the observation of similarly high Ir values in spherule layers and neighboring country rocks was also reported for the S2 layer by Reimold et al. (2000).

Replicate isotope dilution analyses for two CT3 country rock samples, B-SH11 and B-SH19s, resulted in significantly different concentrations for B-SH11 (e.g., 47.6 versus 0.4 ppb Ir and 192 versus 6 ppb for Pt), but similar values for the B-SH19s replicates (e.g., 2328
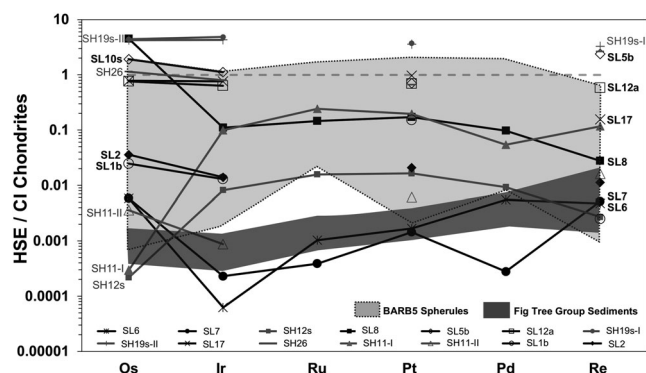

Fig. 2. Highly siderophile element patterns for samples of the CT3 layers normalized to CI values of Palme and Jones (2003). Analyzed spherule layers are shown as black lines, and gray lines show the analyzed country rock samples. The dark gray area represents Fig Tree Group sediments from the BGB (Siebert et al. 2005) and the light gray area presents BARB5 spherule samples from Schulz et al. (2017).

versus 2057 ppb Ir and 3660 versus 3497 ppb for Pt). This might result from an inhomogeneous distribution of HSE carrier phases in the bulk sample powder and exemplifies that such a nugget effect may be more significant for samples at the low-ppb HSE level (B-SH11) compared to samples at the high-ppb HSE level (B-SH19s).

The influence of the proposed inhomogeneous distribution of the HSE carrier phases in the bulk rock powder on measured concentrations between replicates is also our preferred interpretation for concentration differences between data obtained by different techniques. Table 1 shows isotope dilution-generated Os and/or Ir abundance data for some samples in comparison with data obtained by Ozdemir et al. (2017), who used instrumental neutron activation analysis (INAA). In each case separate aliquots of approximately the same weight were analyzed (between ~50 and ~200 mg) with the different techniques. Again, comparably "high-HSE samples" from both lithologies (spherule layer material versus country rock samples; e.g., B-SH19s, B-SL5b) show almost no marked differences in the Os and Ir concentrations between the different replicates (B-SH11 and B-SH19s) and techniques (INAA and isotope dilution) applied. However, samples (e.g., B-SL6, B-SL7) from comparably "low-HSE samples" in some cases exhibit significant differences of up to an order of magnitude between different techniques, although mostly yielding consistent results (e.g., A-SL1b, A-SL2).

Figure 2 shows CI-normalized HSE abundance diagrams for all analyzed CT3 samples. CT3 samples with the highest HSE abundances (B-SL5b, B-SL10s, B-SH19-I/II, B-SL12a, C-SL17, and C-SH26) exhibit a

Table 2. HSE interelement ratios for CT3 samples.

Layer	Os/Ir	Ru/Ir	Pt/Ir	Pd/Ir	Cr/Ir[b]	Os/Pt	Os/Re	Ir/Pt	Re/Pt	Ru/Pd
A-SL1b	2.014		23.92		60.06	0.084	125.1	0.042	0.001	
A-SL2	2.693		3.052		81.55	0.882	40.22	0.328	0.022	
B-SL5b	1.409		1.956	2.437	3.554	0.720	47.41	0.511	0.015	
B-SL6	98.66	23.33	55.00	102.0	25100	1.794	15.58	0.018	0.115	0.229
B-SH11-I	0.003	3.471	4.036	0.632	1.898	0.001	0.032	0.248	0.024	5.496
B-SH11-II	4.333		14.33		215.2	0.302	2.800	0.070	0.108	
B-SL7	26.90	2.364	12.91	1.364	4081	2.085	14.09	0.077	0.148	1.733
B-SH12s	0.028	2.743	4.106	1.315	9.758	0.007	1.000	0.243	0.007	2.085
B-SL8	43.03	1.882	3.191	1.023	34.21	13.48	2055	0.313	0.007	1.840
B-SL10s	1.802		1.288		3.914	1.399	10.15	0.776	0.138	
B-SL12a	1.258		2.224		0.432	0.566	16.56	0.450	0.034	
B-SH19s-I	0.958		1.572		3.934	0.609		0.636		
B-SH19s-II	1.042		1.700		4.454	0.613	16.44	0.588	0.037	
C-SL17	1.082		2.592		22.97	0.417	63.41	0.386	0.007	
C-SH26	1.501		1.684		4.394	0.891	5.493	0.594	0.162	
Chondrites[a]	~1.005–1.291	~1.431–1.691	~1.868–2.367	~0.985–1.728	~4.415–10.72	~0.476–0.614	~9.749–15.41	~0.422–0.535	~0.038–0.054	~0.906–1.494

[a]Data for chondrites from Fischer-Gödde et al. (2010).
[b]Cr data for CT3 samples from Ozdemir et al. (2017) and for chondrites from Tagle and Berlin (2008).

tendency toward less fractionated patterns when compared to the samples with the lowest HSE concentrations. Osmium/Ir and Pt/Ir ratios (as summarized in Table 2), for example, vary from 0.03 to 98.66 and from 3.05 to 14.33 for "low-HSE samples" (e.g., samples A-SL1b, A-SL2, B-SL6, B-SH11, B-SL7, and B-SH12s) and from 0.95 to 1.80 for Os/Ir and from 1.28 to 2.59 for Pt/Ir for "high-HSE-samples" (e.g., samples B-SL5b, B-SH13, B-SL10s, B-SL12a, BSH19s, C-SL17, and C-SH26).

Osmium Isotope Signatures

The $^{187}Os/^{188}Os$ ratios vary from ~0.11 to ~0.16 in spherule layer samples and from ~0.108 to ~1.12 in country rocks. Thus, spherule layer samples always exhibit low, near-chondritic $^{187}Os/^{188}Os$ isotope signatures (e.g., ~0.129 for mantle- or ~0.126 to 0.128 for chondrite-like values; Shirey and Walker 1998), whereas country rocks vary from similarly low values to typical crustal signatures (~1.4; Peucker-Ehrenbrink and Jahn 2001). Such crustal values also cover the average (nonimpact-related) Fig Tree Group sediment ^{187}Os signatures (Siebert et al. 2005). Notably, the lowest $^{187}Os/^{188}Os$ ratio in this study was measured for country rock sample B-SH13 with a value of ~0.108; see Table 1. The lack of a clear distinction between ^{187}Os signatures in spherule layer samples and country rocks is similar to what is observed for the HSE contents in the same samples (which show maximum concentrations in both lithologies).

For comparison, it should be noted that the least radiogenic $^{187}Os/^{188}Os$ ratio reported for (nonimpact-related) sediments from any other sedimentary unit within the Barberton Greenstone Belt (e.g., Moodies Group, Manjeri Formation) is ~0.29 (Siebert et al. 2005). Furthermore, the only lithology that exhibits similarly low $^{187}Os/^{188}Os$ ratios compared to the least radiogenic CT3 samples are volcanic rocks from the Onverwacht Group, especially the komatiites. However, komatiites from the Barberton area are completely unrelated to the CT3 core and have, in contrast to CT3 samples, HSE concentrations in the "low-ppb" level ($^{187}Os/^{188}Os$ ratios vary from ~0.1048 to ~0.1970, and Os and Ir contents varying from 1.30 to 1.40 ppb; Puchtel et al. [2009, 2014] and Connolly et al. [2011]).

In contrast to the ^{187}Os signatures, the $^{187}Re/^{188}Os$ isotope ratios display a dichotomy between spherule layer samples (values ranging from ~0.002 to ~0.338) and country rocks (~0.290 to ~168). Thus, the CT3 country rock samples, on average, mirror and exceed typical $^{187}Re/^{188}Os$ ratios of (not impact-related) Fig Tree Group sediments, which range from ~0.4 to ~9 (Siebert et al. 2005). Interestingly, the complementarity of the $^{187}Re/^{188}Os$ values between the CT3 lithologies (lower in spherule samples, higher in country rocks) is comparable to the behavior of the respective ratios in the BARB5 core. Country rocks intercalating the four BARB5 spherule layers are generally devoid of spherules, represent Fig Tree Group metasediments, and exhibit $^{187}Re/^{188}Os$ ratios between ~0.19 and 0.31 (Schulz et al. 2017). In contrast, $^{187}Re/^{188}Os$ ratios for BARB5 spherule samples range from ~0.01 to ~0.15 (Schulz et al. 2017). This distinctive Re/Os isotope dichotomy between country rocks and spherule layers, now confirmed for BARB5 and CT3 samples, might be
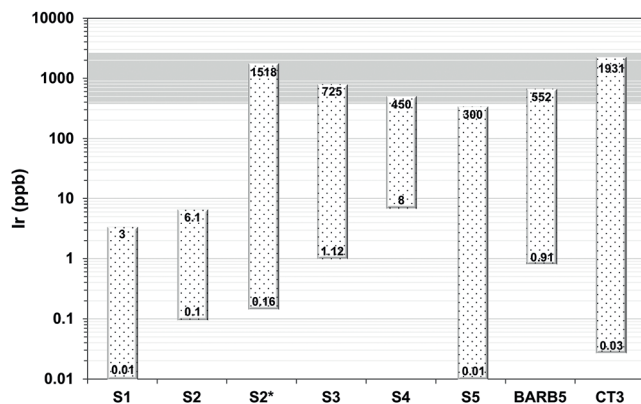
Fig. 3. Maximum and minimum Ir concentrations of early Archean spherule layers from the BGB. Data for S1 to S5 from Lowe et al. (2003, 2014), S2* data from Reimold et al. (2000) and BARB5 data from Schulz et al. (2017). The shaded background shows maximum and minimum Ir abundances of chondrites; data from Tagle and Berlin (2008).

a result of processes that are directly related to the impact event (see Discussion section).

Back-calculated (to an age of ~3.2 Ga; Brandl et al. 2006) $^{187}Os/^{188}Os$ ratios ($^{187}Os/^{188}Os_i$) range from ~0.1068 to ~0.1291 for spherule layer samples and from ~0.1088 to ~0.1655 for the country rock samples, reflecting non-isochronous behavior. Importantly, the chondritic $^{187}Os/^{188}Os$ initial ratio (at ~3.2 Ga) is ~0.105 (Shirey and Walker 1998). Therefore, all CT3 samples exhibit either near-chondritic or slightly superchondritic initial $^{187}Os/^{188}Os$ ratios. Again, comparable results were found for samples from the BARB5 core (Schulz et al. 2017).

DISCUSSION

Meteoritic Admixture and Secondary Processes

As already noted by Ozdemir et al. (2017), an extraterrestrial contribution to the CT3 samples is indicated by petrographic and geochemical observations, especially the high abundances of Os and Ir. The refined and extended data set for HSE presented in this study further strengthens this conclusion. Notably, the maximum HSE abundances presented here (peak values for Ir and Os of 1931 ppb and 2721 ppb, respectively) are the highest ever reported for spherule layers so far.

Figure 3 shows the ranges of Ir concentrations measured for early Archean spherule deposits from the Barberton Greenstone Belt, in comparison to the range for chondritic meteorites. Only spherule deposits (the S2 layer analyzed by Reimold et al. [2000] and the CT3 spherule layer analyzed in this study and by Ozdemir et al. [2017]) exhibit significantly superchondritic values

(see Fig. 3). Schulz et al. (2017), using trace element plots, provided a comparison of these spherule layers with the BARB5 samples. They concluded that both S2 and CT3 spherule deposits experienced moderate secondary alteration. Syn- and/or postimpact mobilization of the HSE via hydrothermal overprint were highlighted as one contributing factor that could explain the superchondritic total abundances (Koeberl and Reimold 1995; Schulz et al. 2017). However, hydrothermally driven enrichments of HSE of up to chondritic or even superchondritic values from samples already enriched in ET component (near-chondritic HSE levels) are not easy to explain and almost impossible to explain for samples with no ET component at all. We note that such hydrothermal processes would have to accidentally create or preserve near-chondritic interelement ratios (in the case of the CT3 samples those found in the most HSE enriched samples). Also, most spherule layer samples in general (e.g., Schulz et al. 2017) and, especially, the CT3 samples either plot on, or in the direct continuation of, roughly linear HSE correlation trends (see Fig. 4) connecting Fig Tree Group sediments and chondrites. This circumstance would be difficult to achieve coincidentally by hydrothermally driven and contemporaneous mobilization of all HSE. Last, it was experimentally shown that, although evidence for some selective HSE mobility exists (which, if at all, predominantly affects the Pt/Pd budgets in sulfide containing systems; e.g., Wallace et al. 1990; Colodner et al. 1992; Barnes and Liu 2012), mobilization of Ir or Os under the conditions of hydrothermal alteration is difficult to achieve (Keays et al. 1982; Martin 1991).

Instead, we propose that the HSE covariations, shown in Fig. 4, mostly represent mixing trends generated by varying extraterrestrial admixtures to the CT3 samples. Varying meteoritic admixtures also provide the best explanation for the observed trends toward less fractionated HSE patterns for the most HSE enriched CT3 samples (thus, showing near-chondritic interelement ratios). This conclusion is supported by Fig. 5, where Os/Ir ratios are plotted versus Ir contents for all CT3 samples. In addition, highly varying Os/Ir ratios for CT3 samples with comparably low Ir contents (below ~1 ppb) contrast with the narrow trend for Os/Ir ratios defined by CT3 samples with high total Ir contents (high-ppb level). Therefore, and as already noted for other Archean spherule layers, our data imply enormous amounts of meteoritic admixtures of up to 100% (Kyte et al. 2003; discussion in Hofmann et al. 2006; Schulz et al. 2017). Superchondritic total abundances might either be explained by the involvement of impactor material not represented in the known chondrite groups (ranging for, e.g., Ir from ~340 to ~2640 ppb from CI to CB
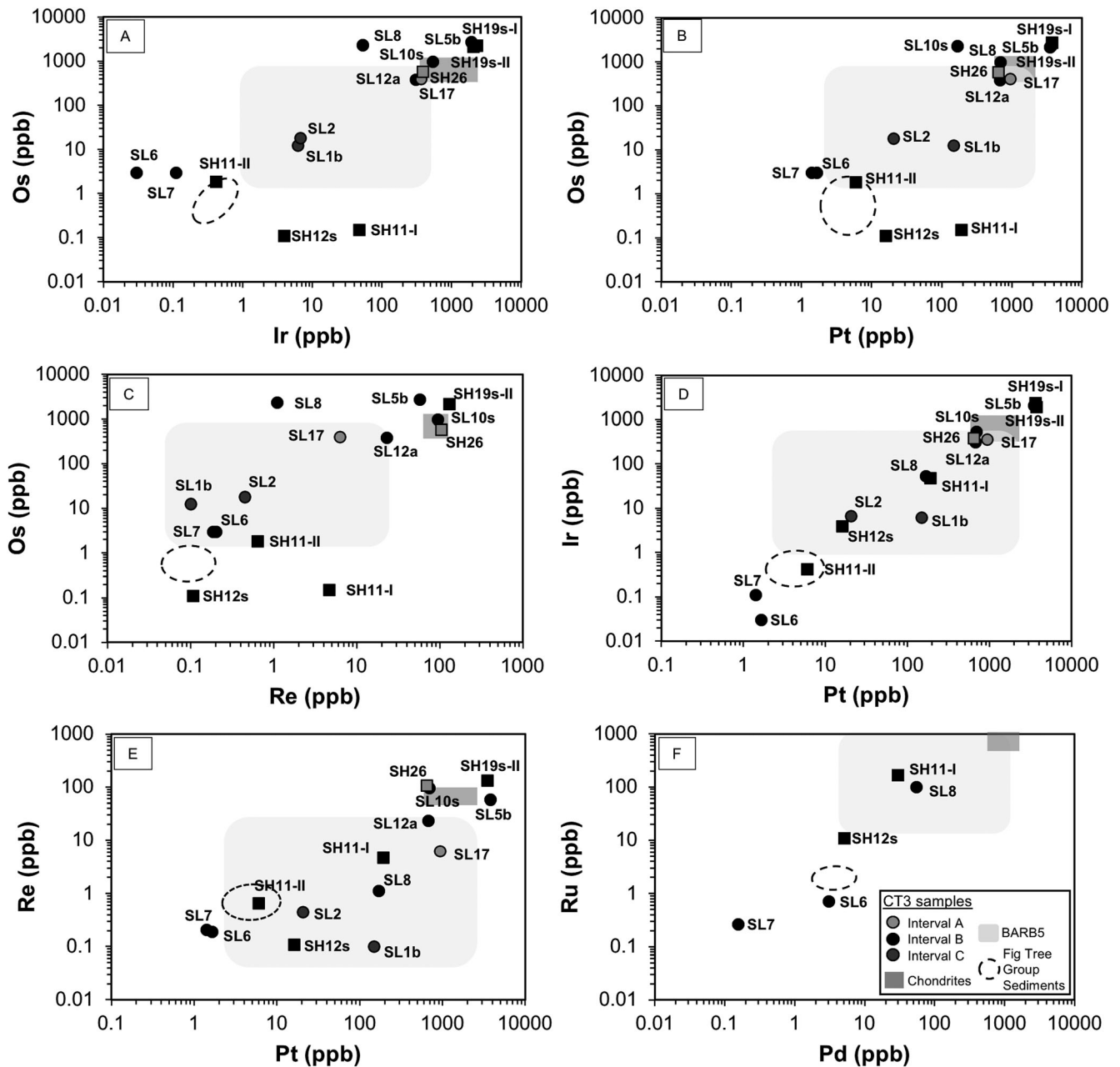
Fig. 4. Interelement diagrams for CT3 layers, Fig Tree Group sediments (data from Siebert et al. 2005), and chondrites (data from Tagle and Berlin 2008). A) Os versus Ir ($R^2 = 0.83$). B) Os versus Pt ($R^2 = 0.77$). C) Os versus Re ($R^2 = 0.67$). D) Ir versus Pt ($R^2 = 0.95$). E) Re versus Pt ($R^2 = 0.63$). F) Ru versus Pd ($R^2 = 0.86$). Also shown are the HSE concentration ranges for Fig Tree Group sediments (Siebert et al. 2005) with dashed ellipses, BARB5 spherule layers (Schulz et al. 2017) with light gray-shaded areas, and chondrites (data from Tagle and Berlin 2008) with dark gray areas. R^2 is the correlation factor for spherule layers samples.

chondrites, respectively, e.g., Tagle and Berlin 2008; Horan et al. 2003), or HSE fractionation and enrichment during generation of the carrier phases inside the impact vapor plume. Postimpact mechanical enrichment of HSE carrier phases in the rocks could also be explored as a possible cause.

Besides the similarities mentioned above, a general difference between the CT3 and BARB5 spherule deposits is the lack of a bimodality in HSE abundances (and ^{187}Os isotope signatures; see discussion below) between spherule layer samples and country rocks in the CT3 samples. Although in the BARB5 core elevated HSE signatures are mostly correlated with the spherule content of the analyzed samples (see discussion in Schulz et al. 2017), maximum HSE concentrations in CT3 samples can be observed in both spherule layers
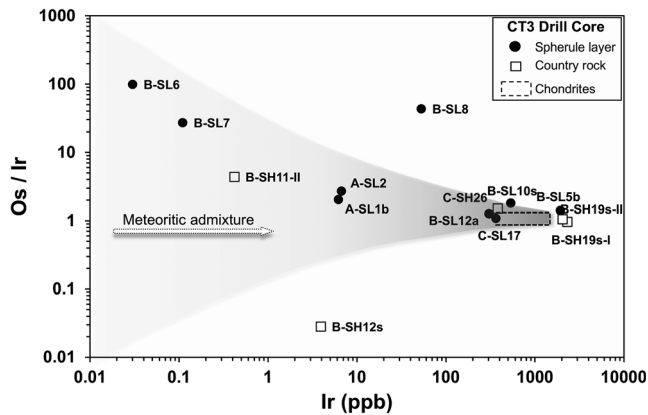
Fig. 5. Diagram of Os/Ir versus Ir for spherule layer and country rock samples from the CT3 drill core, indicating a trend toward chondritic Os/Ir ratios with increasing Ir abundances. Data for chondrites were taken from Tagle and Berlin (2008).

samples (i.e., spherule-groundmass assemblages) and intercalating country rock samples.

If the carrier phases of the meteoritic component in the CT3 core would exclusively be related to spherules, this could argue for the existence of crushed or otherwise fragmented spherules in the CT3 country rocks (which all occur in close vicinity to the next spherule layer). However, Mohr-Westheide et al. (2015, 2018) reported the occurrence of HSE-rich metal alloys associated with Ni-rich chromium spinels within and detached from the spherules (i.e., embedded in the shale groundmass) in the BARB5 and CT3 spherule layer sections. They identified these alloys as the likely carrier phases of the extraterrestrial component. An alternative explanation besides postulating crushed spherules within the country rocks could, thus, be an independent formation of chromium spinels and spherules within the impact vapor plume. In this scenario, chromium spinel could have been associated in the spherules but could also have been incorporated into shales by postimpact wave action in the shallow sea, also noted by Mohr-Westheide et al. (2018). However, the modal abundance of such spinels in our samples might not be high enough to fully explain the amount of meteoritic component present.

The [187]Os Isotope Evidence

Schulz et al. (2017), in their study on the BARB5 spherule layers from the BGB, pointed out that the $^{187}Os/^{188}Os$ signatures (a) are consistently less radiogenic in the spherule-containing samples compared to the spherule-free lithologies; (b) in some spherule-containing samples the measured values are subchondritic; and (c) back-calculated to the time of impact, data never plot

below the chondritic evolution line at that time (in fact the least radiogenic values were exactly chondritic at ~3.4 Ga). The latter fact was interpreted in favor of a chondritic contamination of the samples, whereas the sometimes subchondritic present-day ^{187}Os signatures were interpreted as resulting from Re-loss during or in the wake of the impact event, either by diagenetic mobilization or due to impact vaporization (see discussion in Schulz et al. 2017).

Although lacking an obvious bimodality between the lithologies, $^{187}Os/^{188}Os$ signatures for CT3 rocks behave similarly. The CT3 core samples define a mixing trend between average Fig Tree Group sediments and chondritic endmembers in $^{187}Os/^{188}Os$ versus Os and versus Ir diagrams (see Fig. 6). The ^{187}Os isotope ratios in CT3 spherule samples and most country rocks vary from slightly subchondritic to slightly superchondritic (the present-day minimum value for chondrites is ~0.12; Walker et al. 2002). More radiogenic values are exclusively measured in CT3 country rocks and range in $^{187}Os/^{188}Os$ ratio from ~0.33 (sample B-CH6s, similar to average Fig Tree Group sediments; Siebert et al. 2005) to typical crustal values as high as ~1.13 (for sample B-SH11). None of the CT3 samples exhibit back-calculated (to ~3.2 Ga) ^{187}Os signatures lower than the chondritic value at that time (~0.105; Shirey and Walker 1998). These data further substantiate the postulated chondritic admixture to the CT3 samples. Comparable to the BARB5 samples, subchondritic present-day $^{187}Os/^{188}Os$ ratios CT3 samples (see Table 1) can be reasonably explained by an ^{187}Os isotope evolution with subchondritic Re/Os ratios (Fig. 7). Subchondritic $^{187}Re/^{188}Os$ ratios were reported for BARB5 spherule samples (in contrast to intercalating BARB5 country rocks) by Schulz et al. (2017) in the same way as they are reported here for CT3 spherule layer samples in contrast to average CT3 country rocks. The best explanation is that Re was selectively volatilized during the high-temperature impact event (either in- or outside the impact vapor plume, thereby lowering the Re/Os ratios in the spherule-containing samples).

Duplications of Layers, Number of Separate Events, and the Nature of the Impactor

Based mainly on petrographic and geochemical similarities, Ozdemir et al. (2017) suggested a lower number of individual spherule layers represented by the intersections in the CT3 core, not 17 but only 14. They are assigned to three different intervals A to C, and it was evaluated that these intervals could possibly represent a minimum of three deposits and, thus, impact events. Hoehnel et al. (2018), based on similar investigations and deliberations, concluded that the CT3

Fig. 6. Diagrams of $^{187}Os/^{188}Os$ versus Os and $^{187}Os/^{188}Os$ versus Ir, showing a trend toward less radiogenic Os isotope compositions with increasing (closer to chondritic values) Os and Ir concentrations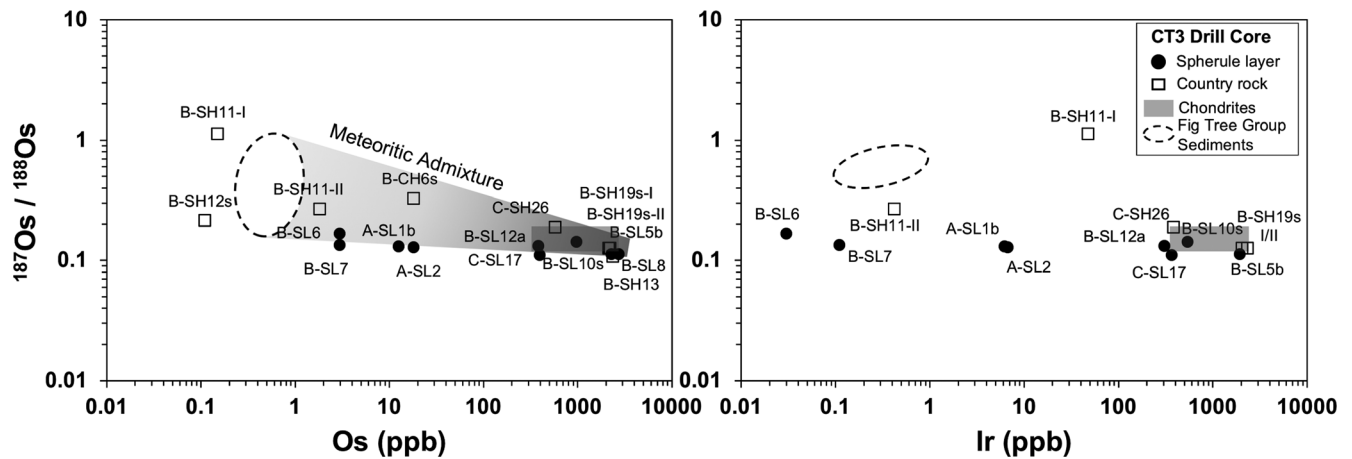. Data for nonimpact-related Fig Tree Group sediments are from Siebert et al. (2005). Chondrite data from Tagle and Berlin (2008).
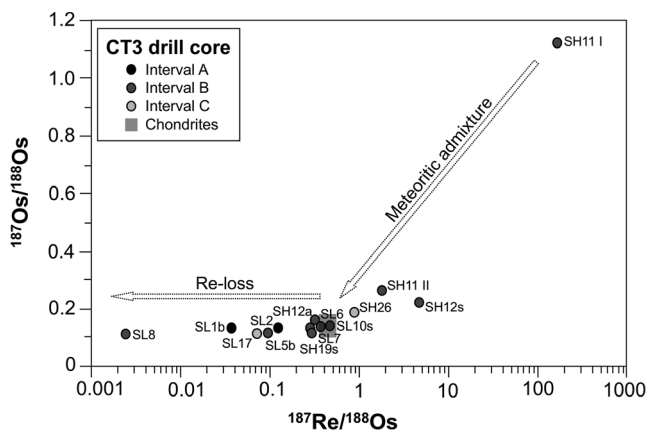

Fig. 7. Diagram of $^{187}Os/^{188}Os$ versus $^{187}Re/^{188}Os$ ratios for the CT3 drill core samples. Chondrite data from Walker et al. (2002). Errors are smaller than symbol sizes.

spherule layers could be variably assigned between 3 to 13 individual impact events. They also emphasized that uncertainty about the actual number of impact events remains due to the complex folding deformation observed throughout the drill core. Obviously, it is difficult to identify tectonic or otherwise duplication of layers and stratigraphic relationships only by having access to drill core sections. However, the most reliable constraints on this issue can, in our mind, be drawn from the fact that one CT3 layer (spherule layer 15 as described by Ozdemir et al. 2017 and Hoehnel et al. 2018) from a core depth of 145 m is unique compared to all others in being the only grain-size sorted layer, which probably was deposited by fallout through a water column. Additionally, there is a ~70 m gap between depth intervals B and C, with no hint at

duplication at the meter scale (Ozdemir et al. 2017). These observations can best be explained by different fallout deposits, most likely representing a minimum number of three individual impact events represented by the CT3 spherule layers. All other claims to propose numbers of impact events, especially regarding those involving different spherule textures and compositions, remain speculative. This was also highlighted by Davatzes (2011), who, based on hydrocode modeling, claimed that impact plumes are heterogeneous in temperature and cooling rate and resulted in fractionation within the plume, leading to spherules of varying compositions and textures (thereby also supporting a conclusion raised above regarding HSE fractionation and superchondritic total abundances).

Data presented in this study (in conjunction with geochemical data presented by Ozdemir et al. 2017) can be interpreted in line with the propositions regarding the number of impact events represented in the CT3 core as mentioned above. Highly siderophile element abundances, for example, are exclusively subchondritic in interval A (with maximum Ir values of up to 6 ppb), subchondritic to superchondritic in interval B (peak Ir concentrations of up to 2300 ppb), and subchondritic to chondritic in interval C (maximum Ir concentrations of 300 ppb). Initial $^{187}Os/^{188}Os$ signatures vary from chondritic to superchondritic in all intervals, showing no clear distinction between the proposed spherule intervals.

Besides the HSE interelement trends discussed in this study, the chondritic initial $^{187}Os/^{188}Os$ isotope signatures at the time of impact/s (~3.2 Ga) represents the most robust evidence for a chondritic impactor. Due to the highly varying HSE concentrations of up to significantly superchondritic values, and due to possible HSE fractionation within the impactor plume(s), it is

not possible to draw any conclusions about the type of chondritic impactor(s) involved.

CONCLUSIONS

The detection of meteoritic signatures in impactites is significant because, under ideal conditions, it allows us to place constraints on the types of impactors and impactor fluxes. In this regard, the Archean spherule layers from the Barberton area (South Africa), representing distal impact ejecta, are unusual as their meteoritic admixtures are the highest ever reported for any impactites worldwide, and they represent (so far) the only accessible impact-related rock record of the early bombardment history of our planet. Previous work performed by Ozdemir et al. (2017), on the recently drilled CT3 core (containing up to 17 spherule layers) provided evidence for an extraterrestrial admixture to the spherule layers and their intercalating country rocks (mostly shales and cherts). The observed superchondritic Os and Ir concentrations in some of these spherule layers led to the present study, which provides a detailed further investigation of the CT3 layers using their HSE concentrations in conjunctions with ^{187}Os isotope signatures. The following conclusions can be drawn:

1. Spherule layer samples (spherule-matrix assemblages) and country rocks (shales and cherts intercalated with the spherule layers) both exhibit HSE concentrations ranging from sub- to superchondritic values;
2. The maximum concentrations in some of the CT3 samples analyzed in this study reach concentrations of up to ~2300 ppb Ir (and ~2700 ppb Os), representing the highest values ever reported for Archean spherule layers from the Barberton area, or in impactites in general;
3. In contrast to the BARB5 layer, HSE concentrations in the CT3 spherule section do not even roughly correlate with spherule density (number of spherules per area). Peak HSE concentrations can be observed in (spherule-free) country rocks and spherule layers. This, together with trace element diagrams for both cores presented by Schulz et al. (2017), point toward significant secondary overprint in the CT3 compared to the BARB5 spherule layer sections;
4. All CT3 samples define rough linear mixing trends connecting impact-unrelated Fig Tree Group sediments with chondrites in HSE interelement diagrams, strongly supporting the existence of varying amounts of an extraterrestrial component in the samples;
5. The presence of near-chondritic or even superchondritic HSE concentrations in spherule samples and country rocks (in close vicinity to the next spherule layer) suggests the presence of fragmented or otherwise crushed spherules in the country rocks, or postdepositional mechanical enrichment of chromium spinel (HSE carrier phases; Mohr-Westheide et al. 2015, 2018).
6. Alternatively, superchondritic HSE abundances might be best a result of fractionation processes within the impact vapor plume, maybe accompanied by postdepositional mechanical or chemical enrichment of HSE carrier phases in the rocks, making quantification of inherited meteoritic admixtures problematic;
7. Initial ^{187}Os isotope signatures of most samples (back-calculated to ~3.2 Ga) range from chondritic (~0.105; Shirey and Walker 1998) to superchondritic (up to 0.165), arguing for a chondritic impactor (or a differentiated asteroid with similar bulk composition, possibly not represented in our present-day meteorite inventory);
8. Present-day ^{187}Os values in some CT3 samples are slightly subchondritic, resulting from isotope evolution with a subchondritic Re/Os ratio, probably resulting from Re-loss at the time of impact via volatilization, or in the wake of the impact event via hydrothermal activity or mechanical enrichment.

Editorial Handling—Dr. Jeffrey Plescia

REFERENCES

Barnes S. J. and Liu W. 2012. Pt and Pd mobility in hydrothermal environments: Evidence from komatiites and

from thermodynamic modelling. *Ore Geology Reviews* 44:49–58.

Birck J. L., Barman M. R., and Capmas F. 1997. Re-Os isotopic measurements at the femtomole level in natural samples. *Geostandards Newsletter* 20:19–27.

Brandl G., Cloete M., and Anhaeusser C. R. 2006. Archaean Greenstone belts. In *The Geology of South Africa*, edited by Johnson M. R., Anhaeusser C. R., and Thomas R. J. Johannesburg, South Africa: Geological Society of South Africa/Council for Geoscience. pp. 9–56.

Brandon A. D., Humayun M., Puchtel I. S., Leya I., and Zolensky M. 2005. Geochemistry: Osmium isotope evidence for an s-process carrier in primitive chondrites. *Science* 309:1233–1236.

Byerly G. R., Lowe D. R., Wooden J. L., and Xie X. 2002. An Archean impact layer from the Pilbara and Kaapvaal cratons. *Science* 297:1325–1327.

Cohen A. S. and Waters F. G. 1996. Separation of osmium from geological materials by solvent extraction for analysis by thermal ionisation mass spectrometry. *Analytica Chimica Acta* 332:269–275.

Colodner D. C., Edward B. A., Edmond J. M., and Thomson J. 1992. Post-depositional mobility of platinum, iridium, and rhenium in marine sediments. *Nature* 358:402–404.

Connolly B. D., Puchtel I. S., Walker R. J., Arenalo R. Jr., Piccoli P. M., Byerly G., Robin-Popieul C., and Arndt N. 2011. Highly siderophile element systematics of the 3.3 Ga Weltevreden komatiites, South Africa: Implications for early Earth history. *Earth and Planetary Science Letters* 311:253–263.

Davatzes A. E. 2011. Impact plume fractionation as indicated by size and mineral diversity in Archean spherules (abstract #1751). 42nd Lunar Planetary Science Conference. CD-ROM.-

Esser B. K. and Turekian K. K. 1993. The osmium isotope composition of the continental crust. *Geochimica et Cosmochimica Acta* 57:3093–3104.

Fischer-Gödde M., Becker H., and Wombacher F. 2010. Rhodium, gold and other highly siderophile element abundances in chondritic meteorites. *Geochimica et Cosmochimica Acta* 74:356–379.

Fritz J., Tagle R., Ashworth L., Schmitt R. T., Hofmann A., Luais B., Harris P. D., Hoehnel D., Özdemir S., Mohr-Westheide T., and Koeberl C. 2016. Nondestructive spectroscopic and petrochemical investigations of Paleoarchean spherule layers from the ICDP drill core BARB5, Barberton Mountain Land, South Africa. *Meteoritics & Planetary Science* 51:2441–2458.

Glass B. P. and Simonson B. M. 2013. *Distal impact ejecta layers. Impact studies.* Berlin, Germany: Springer. 716 p.

Goderis S., Simonson B., McDonald I., Hassler S., Izmer A., Belza J., Terryn H., Vanhaecke F., and Claeys P. 2013. Ni-rich spinels and platinum group element nuggets condensed from a Late Archaean impact vapour cloud. *Earth and Planetary Science Letters* 376:87–98.

Hoehnel D., Reimold W. U., Altenberger U., Hofmann A., Mohr-Westheide T., Ozdemir S., and Koeberl C. 2018. Petrographic and micro-XRF analysis of multiple Archean impact-derived spherule layers in drill core CT3 from the northern Barberton Greenstone Belt (South Africa). *Journal of African Earth Sciences* 138:264–288.

Hofmann A. 2005. The geochemistry of sedimentary rocks from the Fig Tree Group, Barberton greenstone Belt: Implications for tectonic, hydrothermal and surface processes during mid-Archean times. *Precambrian Research* 143:23–49.

Hofmann A., Reimold W. U., and Koeberl C. 2006. Archean spherule layers in the Barberton Greenstone Belt, South Africa: A discussion of problems related to the impact interpretation. In *Processes on the early Earth*, edited by Reimold W. U. and Gibson R. L. *Geological Society of America Special Paper* 405:33–56.

Horan M. F., Walker R. J., Morgan J. W., Grossman J. N., and Rubin A. E. 2003. Highly siderophile elements in chondrites. *Chemical Geology* 196:5–20.

Keays R. R., Nickel E. H., Groves D. I., and McGoldrick P. J. 1982. Iridium and palladium as discriminants of volcanic-exhalative, hydrothermal, and magmatic nickel sulfide mineralization. *Economic Geology* 77:1535–1547.

Koeberl C. 2007. The geochemistry and cosmochemistry of impacts. In *Treatise on geochemistry*, Vol. 1, edited by Davis A. M. Amsterdam, the Netherlands: Elsevier. pp. 1-28–1-52.

Koeberl C. 2014. The geochemistry and cosmochemistry of impacts. In *Planets, asteriods, comets and the solar system*, edited by Davis A. M. Treatise on Geochemistry, 2nd ed., Vol. 2. Amsterdam, the Netherlands: Elsevier. pp. 73–118.

Koeberl C. and Reimold W. U. 1995. Early Archean spherule beds in the Barberton Mountain land, South Africa: No evidence for impact origin. *Precambrian Research* 74:1–33.

Koeberl C. and Shirey S. B. 1997. Re-Os systematics as a diagnostic tool for the study of impact craters and distal ejecta. *Palaeogeography, Palaeoclimatology, Palaeoecology* 132:25–46.

Koeberl C., Claeys P., Hecht L., and McDonald I. 2012. Geochemistry of impactites. *Elements* 8:37–42.

Kyte F. T., Zhou L., and Lowe D. R. 1992. Noble metal abundances in an Early Archean impact deposit. *Geochimica et Cosmochimica Acta* 56:1365–1372.

Kyte F. T., Shukolyukov A., Lugmair G. W., Lowe D. R., and Byerly G. R. 2003. Early Archean spherule beds: Chromium isotopes confirm origin through multiple impacts of projectiles of carbonaceous chondrite type. *Geology* 31:283–286.

Lowe D. R. and Byerly G. R. 1986. Early Archean silicate spherules of probable impact origin, South Africa and Western Australia. *Geology* 14:83–86.

Lowe D. R., Byerly G. R., Asaro F., and Kyte F. T. 1989. Geological and geochemical record of 3400- million- year-old terrestrial meteorite impacts. *Science* 245:959–962.

Lowe D. R., Byerly G. R., Kyte F. T., Shukolyukov A., Asaro F., and Krull A. 2003. Spherule beds 3.47-3.24 billion years old in the Barberton Greenstone Belt, South Africa: A record of large meteorite impacts and their influence on early crustal and biological evolution. *Astrobiology* 3:7–47.

Lowe D. R., Byerly G. R., and Kyte F. T. 2014. Recently discovered 3.42–3.23 Ga impact layers, Barberton Belt, South Africa: 3.8 Ga detrital zircons, Archean impact history, and tectonic implications. *Geology* 42:747–750.

Luguet A., Nowell G. M., and Pearson D. G. 2008. $^{184}Os/^{188}Os$ and $^{186}Os/^{188}Os$ measurements by Negative Thermal ionisation mass spectrometry (N-TIMS): Effects of interfering element and mass fractionation corrections on data accuracy and precision. *Chemical Geology* 248:342–362.

Luguet A., Behrens M., Pearson D. G., König S., and Herwartz D. 2015. Significance of the whole rock Re–Os

ages in cryptically and modally metasomatized cratonic peridotites: Constraints from HSE–Se–Te systematics. *Geochimica et Cosmochimica Acta* 164:441–463.

Martin C. E. 1991. Osmium isotopic characteristics of mantle-derived rocks. *Geochimica et Cosmochimica Acta* 55:1421–1434.

Mohr-Westheide T., Reimold W. U., Fritz J., Koeberl C., Salge T., Hofmann A., and Schmitt R. T. 2015. Discovery of extraterrestrial component carrier phases in Archean spherule layers: Implications for estimation of Archean bolide sizes. *Geology* 43:299–302.

Mohr-Westheide T., Greshake A., Wirth R., and Reimold W. U. 2018. Transmission electron microscopy of impact-generated platinum group element alloys from Barberton spherule layers: New clues to their formation. *Meteoritics & Planetary Science* 53:1516–1536.

Ozdemir S., Schulz T., Koeberl C., Reimold W. U., Mohr-Westheide T., Hoehnel D., and Schmitt R. T. 2017. Early Archean spherule layers from the Barberton Greenstone Belt, South Africa: Mineralogy and geochemistry of the spherule beds in the CT3 drill core. *Meteoritics & Planetary Science* 52:2586–2631.

Palme H. 1982. The identification of projectiles of large terrestrial impact craters and some implications for the interpretation of Ir-rich cretaceous-tertiary boundary layers. In *Geological implications of impacts of large asteroids and comets on the Earth*, edited by Silver L. T. and Schultz P. H. *Geological Society of America Special Paper* 190:223–233.

Palme H. and Jones A. 2003. Solar system abundances of the elements. In *Treatise on geochemistry*, edited by Holland H. D. and Turekian K. K. Amsterdam, the Netherlands: Elsevier. pp. 41–61.

Pearson D. G. and Woodland S. J. 2000. Solvent extraction/anion exchange separation and determination of PGE (Os, Ir, Pt, Pd, Ru) and Re-Os isotopes in geological samples by isotope dilution ICP-MS. *Chemical Geology* 165:87–107.

Peucker-Ehrenbrink B. and Jahn B. 2001. Rhenium-osmium isotope systematics and platinum group element concentrations: Loess and the upper continental crust. *Geochemistry, Geophysics, Geosystems* 2:22. https://doi.org/10.1029/2001gc000172.

Puchtel I. S., Walker R. J., Anhaeusser C. R., and Gruau G. 2009. Re-Os isotope systematics and HSE abundances of the 3.5 Ga Schauenburg komatiites, South Africa: Hydrous melting or prolonged survival of primordial heterogeneities in the mantle? *Chemical Geology* 262:355–369.

Puchtel I. S., Walker R. J., Touboul M., Nisbet E. G., and Byerly G. R. 2014. Insights into early Earth from the Pt-Re-Os isotope and highly siderophile element abundance systematics of Barberton komatiites. *Geochimica et Cosmochimica Acta* 125:394–413.

Reimold W. U. and Koeberl C. 2014. Impact structures in Africa: A review. *Journal of African Earth Sciences* 93:57–175.

Reimold W. U., Koeberl C., Johnson S., and McDonald I. 2000. Early Archean spherule beds in the Barberton Mountain Land, South Africa: Impact or terrestrial origin? In *Impacts and the early Earth*, edited by Gilmour I. and Koeberl C. *Lecture Notes in Earth Sciences* 91:117–180.

Schulz T., Koeberl C., Luguet A., Van Acken D., Mohr-Westheide T., Ozdemir S., and Reimold W. U. 2017. New constraints on the Paleoarchean meteorite bombardment of the Earth—Geochemistry and Re-Os isotope signatures of the BARB5 ICDP drill core from the Barberton Greenstone Belt, South Africa. *Geochimica et Cosmochimica Acta* 211:322–340.

Shirey S. B. and Walker R. J. 1998. The Re-Os isotope system in cosmochemistry and high-temperature geochemistry. *Annual Review of Earth and Planetary Sciences* 26:423–500.

Shukolyukov A., Kyte F. T., Lugmair G. W., Lowe D. R., and Byerly G. W. 2000. The oldest impact deposits on Earth—First confirmation of an extraterrestrial component. In *Impacts and the early Earth*, edited by Gilmour I. and Koeberl C. *Lecture Notes in Earth Sciences* 91:99–115.

Siebert C., Kramers J. D., Meisel T., Morel P., and Nägler T. F. 2005. PGE, Re-Os, and Mo isotope systematics in Archean and early Proterozoic sedimentary systems as proxies for redox conditions of the early Earth. *Geochimica et Cosmochimica Acta* 69:1787–1801.

Simonson B. M. 1992. Geological evidence for a strewn fied of impact spherules in the early Precambrian Hamersley Basin of Western Australia. *Geological Society of American Bulletin* 104:829–839.

Simonson B. M., Koeberl C., McDonald I., and Reimold W. U. 2000. Geochemical evidence for an impact origin for a Late Archean spherule layer, Transvaal Supergroup, South Africa. *Geology* 28:1103–1106.

Simonson B. M., McDonald I., Shukolyukov A., Koeberl C., Reimold W. U., and Lugmair G. W. 2009. Geochemistry of 2.63-2.49 Ga impact spherule layers and implications for stratigraphic correlations and impact processes. *Precambrian Research* 175:51–76.

Smoliar M. I., Walker R. J., and Morgan J. W. 1996. Re-Os ages of group IIA, IIIA, IVA, and IVB iron meteorites. *Science* 271:1099–1102.

Tagle R. and Berlin J. 2008. A database of chondrite analyses including platinum group elements, Ni Co, Au, and Cr: Implications for the identification of chondritic projectiles. *Meteoritics & Planetary Science* 43:541–559.

Van Acken D., Brandon A. D., and Humayun M. 2011. High-precision osmium isotopes in enstatite and Rumuruti chondrites. *Geochimica et Cosmochimica Acta* 75:4020–4036.

Walker R. J., Horan M. F., Morgan J. W., Becker H., Grossman J. N., and Rubin A. E. 2002. Comparative ^{187}Re-^{187}Os systematics of chondrites: Implications regarding early solar system processes. *Geochimica et Cosmochimica Acta* 66–23:4187–4201.

Wallace M. W., Gostin V. A., and Keays R. R. 1990. Acraman impact ejecta and host shales: Evidence for low temperature mobilization of iridium and other platinoids. *Geology* 18:132–135.